

# Can the fluorescence quantum yield be enhanced by introducing the benzene ring to the blue fluorescent protein chromophore?

Received Oct.25, 2018,  
Accepted Nov. 30, 2018,

DOI: 10.4208/jams.102518.113018a

<http://www.global-sci.org/jams/>

Bing Liu (刘冰)<sup>1</sup>, Qi Wei(魏琦)<sup>1</sup>, Ruihu Tao(陶瑞虎)<sup>1</sup>, Pengjie Gao(高鹏杰)<sup>1</sup>, Panwang Zhou(周潘旺)<sup>2</sup>, Chaozhuo Liu(刘超卓)<sup>1</sup>, Li Zhao(赵莉)<sup>1,\*</sup>

**Abstract.** The green fluorescent protein (GFP) has been widely used in biochemical and biological fields for its strong fluorescence emitting property. The effective fluorescence emitting property lies in its chromophore P-HBI. Compared with GFP, the low fluorescence quantum yield (0.2 vs. 0.8 of GFP) of the wild blue fluorescent protein (BFP) restricts its extensive applications. In order to enhance the fluorescent quantum yield of BFP, numerous attempts have been executed to modify the molecular configuration such as introducing the intramolecular hydrogen bond (IHB) or benzene ring to the parent structure. In the present work, we employed the high-level quantum chemistry calculation method CASSCF to investigate the excited state deactivation mechanism of 4-BFP, which is a newly synthesized BFP chromophore derivative by introducing a benzene ring to the five-membered heterocycle attempting to increase the fluorescence quantum yield. By combination of the optimization of stable electronic structures, scanning of potential energy surfaces and construction of energy profile, we found that the fluorescent quantum yield could not be enhanced for the 4-BFP molecule. One minimum energy conical intersection was located between the S1 and S0 states, which could act as the gateway for the 4-BFP to funnel to the ground state by the internal conversion process. The current work could provide fundamental guide for further molecular structure modification or improvement to enhance the fluorescent quantum yield of BFP analogues.

**Keywords:** Fluorescence; Excited state; Decay process; Photoisomerization.

## 1. Introduction

In 1962, the discovery of the green fluorescent protein in jellyfish *Aequorea Victoria* has been recognized as a milestone in the biochemistry and biology fields.[1-4] The fluorescence quantum yield of the wild GFP reached up to 0.8[1, 4, 5]. Such high and strong fluorescence emitting property makes it very suitable for widespread applications, such as acting as the biomarkers or biosensors to track the gene expression [1, 6, 7], protein or cancer cell localization[8]. Based on the wide applications of the GFP and growing increase for different visualization abilities, many GFP variants such as red LSSmKate2 protein[9], HcRed protein[10, 11], mKeima[12], Photoactive Yellow Protein[13-15], and Kindling Fluorescent Protein[16, 17] have been synthesized. The Y66H mutant of the GFP can emit blue fluorescence, and thus been termed as blue fluorescent protein (BFP), which can act as a donor molecule for the fluorescence resonant energy transfer (FRET).[18] The fluorescence quantum yield of the BFP is much lower than that of the GFP (0.2 vs. 0.8),[19] which has stunted its extensive applications. In addition, no fluorescence was detected when the BFP is inactivation or the chromophore is isolated. It has been proposed that the low fluorescence quantum yield lies in the conformation torsional motion of the

chromophore, which could drive the system decay to the ground state by internal conversion process. The underlying mechanism has been thoroughly investigated theoretically [19, 20]. Numerous attempting has been executed such as increasing the hydrostatic pressure [21], decreasing the temperature [19, 22] and modifying the molecular structure aiming to enhance its fluorescence quantum yield. The changes on the external environmental can remarkably enhance the fluorescence emitting of the BFP.[21] Nowadays, researchers paid attention to synthesizing new compounds by introducing chemical groups to the parental BFP chromophore. Fang and co-workers [23] synthesized the 2-BFP ((4Z)-4-[(1H-imidazol-2-yl)methylene]-1-methyl-2-phenyl-1Himidazol5(4H)-one) by introducing an intramolecular hydrogen bond, and 4-BFP by introducing a benzene ring to the wild BFP chromophore. It was found that the intramolecular hydrogen bond of 2-BFP could increase the fluorescence emitting and

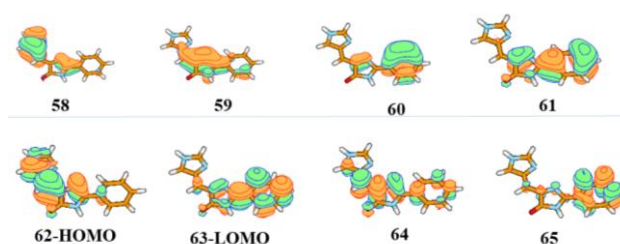


**Figure 1:** The active spaces included in SA2-CASSCF(10,8) calculation method for the 4-BFP molecule on the ground state.

<sup>1</sup>College of Science, China University of Petroleum (East China), Qingdao, 266580, Shandong, P. R. China.

<sup>2</sup>State Key Laboratory of Molecular Reaction Dynamics, Dalian Institute of Chemical Physics, Chinese Academy of Sciences, Dalian 116023, P. R. China

Corresponding authors: Email: zhaoli282@upc.edu.cn

leads to a dual fluorescence property. The underlying mechanism has been proposed by Cui's group[24]. However, does the fluorescence quantum yield of the 4-BFP molecule increase similar to that of the 2-BFP? What is the decay mechanism of the 4-BFP system when being excited to the  $S_1$  state? The introduced benzene ring can prohibit the photoisomerization process because of the steric effect? The answers to these questions are important for deep understanding of the excited state dynamics behavior of the BFP related systems and further design of applicable fluorescence analogues. Motivated by this, in the present work we employed the high-level electronic structure calculations to investigate the excited state dynamics behavior of the 4-BFP system. Our calculation results suggested that different from the 2-BFP, the internal conversion process rather than the fluorescence emitting dominates the deactivation process of the 4-BFP, and the decay reaction coordinate was driven by the photoisomerization process of the bridging bond.

## 2. Calculation Methods

The optimization of the stable structures of the 4-BFP molecule on the ground state ( $S_0$ ) and the lowest singlet excited state ( $S_1$ ), and the minimum energy conical intersections (MECIs) between the  $S_0$  and  $S_1$  states were optimized by means of state averaged complete active space self-consistent field (CASSCF) method. Two electronic states included in the average procedure were executed with the equal weights. Considering the computational cost of the CASSCF method, we need to choose a proper active space which can not only provide accurate results but also spend less computational resources. For the targeted system, the active space is composed of 10 electrons in 8 orbitals eliminating that with occupations close to 2.00 and 0.00. All the included orbitals are  $\pi$  type. More information about the orbitals

**Table 1** Key geometrical information (bond lengths (Å) and dihedral angles (degree)) of the equilibrium structures on the  $S_0$  and  $S_1$  states and the MECI of 4-BFP optimized at SA2-CASSCF(10,8)/6-31G\*\* level.

Geo.	C2C3	C3C4	N1C2C3	C2C3C4	C3C4N5	N1C2C3C4	C2C3C4N5
$S_0$ -min	1.346	1.458	129.8	129.6	125.7	0.0	0.0
$S_1$ -min	1.419	1.429	131.4	126.9	125.5	0.0	0.0
MECI1	1.438	1.404	120.7	127.9	130.6	111.0	-2.79

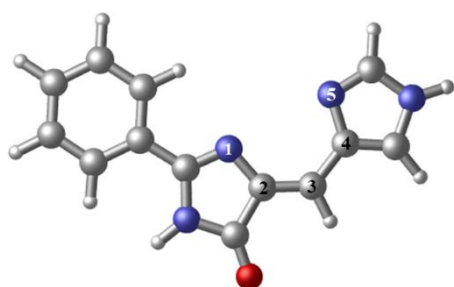


**Figure 2:** The most stable structure and numbering scheme of the 4-BFP molecule optimized at the SA2-CASSCF(10,8)/6-31G\*\* level, in this figure and others, blue: N; grey: C; red: O; and white: H.

involved in the active spaces can be found in **Figure 1**. The 6-31G\*\* basis set was employed for all atoms. The energy profile connecting the Franck-Condon point and the MECI constructed by the linearly interpolated internal coordinate (LIIC) was calculated with the SA2-CASSCF(10,8)/6-31G\*\* method. In addition, the two-dimensional potential energy surfaces of the  $S_0$  and  $S_1$  states as functions of the N1CCC and CCCN5 dihedral angles were calculated at the SA2-CASSCF(10,8)/6-31G\* level. All the electronic structure calculations were executed with the Molpro 2010.1 program package.[25]

## 3. Results and discussion

### 3.1 Geometry Optimization

The equilibrium structure of the 4-BFP system on the ground state together with the numbering scheme is displayed in **Figure 2**. The dihedral angles N1C2C3C4 and C2C3C4N5 are used to quantify the twisting motion around the bridging bonds C2C3 and C3C4, respectively. The most relevant geometrical parameters of the stable structures on the  $S_0$  and  $S_1$  states optimized at the SA2-CASSCF (10,8) /6-31G\*\* level are summarized in **Table 1**. As shown, the  $S_0$ -min and  $S_1$ -min are planar structures, characterized by the torsional angles N1C2C3C4 and C2C3C4N5 of 0.0°. The geometrical differences between  $S_0$ -min and  $S_1$ -min mainly lie in the bond lengths of C2C3 and C3C4. Compared with  $S_0$ -min, the C2C3 length of the  $S_1$ -min stretched from 1.346 Å to 1.419 Å, while the C3C4 bond length shrunk from 1.458 Å to 1.429 Å. The bond angles N1C2C3, C2C3C4 and C3C4N5 exhibit little change. The longer bond length of C2C3 will decrease the steric hindrance between the two five-membered heterocycles, and thus facilitate the twisting motion around the C2C3 bond. One MECI was located on the  $S_1/S_0$  crossing seam as displayed in **Figure 3**. The relevant geometrical parameters are also summarized in **Table 1**. Obviously, the C2C3 bond length further stretched to

**Table 2** The vertical excitation energy (in eV) to the  $S_1$  state and relative energies between  $S_0$ -min,  $S_1$ -min and MECI calculated at the SA2-CASSCF(10,8)/6-31G\*\* level.

Geo.	VE	RE <sup>1</sup>	RE <sup>2</sup>
$S_0$ -min	5.55	0.00	0.00
$S_1$ -min	3.25	1.34	-0.96
MECI	0.00	4.23	-1.30

<sup>1</sup> Energies relative to ground state energy of  $S_0$ -min.

<sup>2</sup> Energies relative to  $S_1$  state energy of  $S_0$ -min geometry.

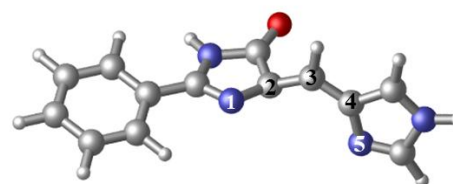


**Figure 3:** The minimum energy conical intersection between the  $S_0$  and  $S_1$  states located at the SA2-CASSCF(10,8)/6-31G\*\* level.

1.438 Å, while the C3C4 bond shrunk to 1.404 Å compared with  $S_1$ -min. Such further bond length changes could make the twisting motion around the C2C3 bond more facile, which can be confirmed by the dihedral angle value of N1C2C3C4 increasing from 0.0° to 111.0°. For the bond angles, N1C2C3 decreased about 10° to 120.7°, while C3C4N5 increased from 125° to 130°.

### 3.2 Energy property

The vertical excitation energy to the  $S_1$  state and the relative energies between the  $S_0$ -min,  $S_1$ -min and MECI calculated at the CASSCF level were collected in **Table 2**. The  $S_0$ - $S_1$  vertical excitation energy is calculated to be 5.55 eV. The  $S_1$  state energy of the  $S_1$ -min is 3.25 eV, which is about 2.3 eV below the Franck-Condon point. Most importantly, the MECI was located about 0.4 eV below the  $S_1$ -min, indicating that the conical intersection region is energetically accessible when the system was being excited to the  $S_1$  state. In order to confirm the role of the MECI played in the excited state decay process, the one-dimensional energy profile connecting the Franck-Condon point and the MECI was constructed by the LIIC method shown in **Figure 4**. As displayed, it is a non-barrier

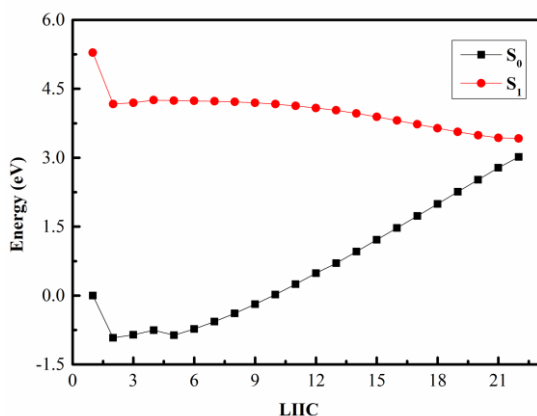


**Figure 4:** The energy profile connecting the Franck-Condon point and the MECI by the LIIC method calculated at the SA2-CASSCF (10,8)/6-31G\*\* level.

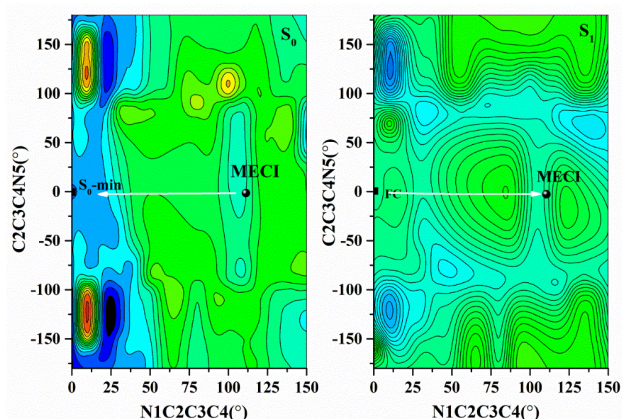


**Figure 5:** The potential energy surfaces of the  $S_1$  and  $S_0$  states as functions of the N1C2C3C4 and C2C3C4N5 dihedral angles. The marks are the  $S_0$ -min, Franck-Condon point (FC) and the MECI as labeled, and the white arrows are the instructions of the reaction coordinates.

decay process on the  $S_1$  state starting from the Franck-Condon point. That is, the topology structure of the excited state will contribute the system to approach the conical intersection region. Afterwards, the system can then funnel to the ground state by the MECI region and complete the deactivation process. In order to provide a more detailed picture of the decay process, we scanned the potential energy surfaces (PESs) of the  $S_1$  and  $S_0$  states as functions of the N1C2C3C4 and C2C3C4N5 dihedral angles. The PESs, the marked critical geometry points and relaxation coordinates are shown in **Figure 5**. As displayed, the deactivation process was dominated by the C2C3 bond rotation process when being excited to the  $S_1$  state. After approaching the conical intersection seam, the system can then funnel to the ground state by internal conversion process. Afterwards, the system continues to adjust geometries to return back to the  $S_0$ -min region and complete the whole deactivation process. Based on the results mentioned above, it is not hard to summarize the deactivation process of 4-BFP system as follows:

$S_0$ -min  $\rightarrow$  FC point  $\rightarrow$  MECI  $\rightarrow$   $S_0$ -min

## 4. Conclusions

In the current work, we employed the high-level quantum chemistry method CASSCF to investigate the deactivation mechanism of the 4-BFP system under vacuum by optimizing the stable geometries, constructing the energy profiles, and scanning the potential energy potential surfaces. One minimum conical intersection was located between the  $S_1$  and  $S_0$  seam, which can act as the gateway for the system to decay to the ground state. The topological structures of energy profile and the potential energy surfaces indicated an effective non-barrier relaxation process on the  $S_1$  state. Therefore, the fluorescence quantum yield of 4-BFP could not be enhanced by introducing the benzene ring to the parent BFP chromophore. The current work can provide theoretical guide for further design or improvement of fluorescent chromophore to increase the fluorescence quantum yield and widen applications.

## Acknowledgments

We are grateful to the National Natural Science Foundation of China (No. 21803077), Fundamental Research Funds for the Central Universities (No. 18CX02025A) and University Student Innovation Project of UPC (No. 20171489) for financial support.

## References

- [1] Chalfie M, Tu Y, Euskirchen G, Ward W W and Prasher D C 1994 Science 263 802
- [2] Schwille P, Kummer S, Heikal A A, Moerner W E and Webb W W 2000 Proc. Natl. Acad. Sci. U. S. A. 97 151
- [3] Zimmer M 2002 Chem. Rev. 102 759
- [4] Lippincott-Schwartz J, Snapp E and Kenworthy A 2001 Nature Rev. Mol. Cell Biol. 2 444

- [5] Chishima T, Miyagi Y, Wang X, Yamaoka H, Shimada H, Moossa A R and Hoffman R M 1997 *Cancer Res.* 57 2042
- [6] Prasher D C, Eckenrode V K, Ward W W, Prendergast F G and Cormier M J 1992 *Gene* 111 229
- [7] Inouye S and Tsuji F I 1994 *FEBS Lett.* 341 277
- [8] Tsien R Y, Bacskai B J and Adams S R 1993 *Trends Cell Biol.* 3 242
- [9] Randino C, Nadal-Ferret M, Gelabert R, Moreno M and Lluch J M 2013 *Theor. Chem. Acc.* 132
- [10] Sun Q, Li Z, Lan Z, Pfisterer C and Doerr M 2012 *Phys. Chem. Chem. Phys.* 14 11413
- [11] Subach F V and Verkhusha V V 2012 *Chem. Rev.* 112 4308
- [12] Henderson J N, Osborn M F, Koon N, Gepshtein R, Dan Huppert and Remington S J 2009 *J. Am. Chem. Soc* 131 13212
- [13] Garcia-Prieto F F, Munoz-Losa A, Fdez Galvan I, Sanchez M L, Aguilar M A and Martin M E 2017 *J. Chem. Theory. Comput.* 13 737
- [14] Pande K, Hutchison C D M, Groenhof G, Aquila A, Robinson o S, Tenboer J, Basu S, Boutet S, DePonte D P, Liang M, White T A, Zatsepin N A, Yefanov O, Morozov D, Oberthuer D, Gati C, Subramanian G, James D, Zhao Y, Koralek J, Brayshaw J, Kupitz C, Conrad C, Roy-Chowdhury S, Coe J D, Metz M, Xavier P L, Grant T D, Koglin J E, Ketawala G, Fromme R, Šrajer V, Henning R, Spence J C H, Ourmazd A, Peter Schwander, Weierstall U, Frank M, Fromme P, Barty A, Chapman H N, Moffat K, Thor J J v and Schmidt M 2016 *Science* 352 725
- [15] Nakamura R and Hamada N 2015 *J. Phys. Chem. B* 119 5957
- [16] Grigorenko B L, Polyakov I V, Savitsky A P and Nemukhin A V 2013 *J. Phys. Chem. B* 117 7228
- [17] Addison K, Heisler I A, Conyard J, Dixon T, Bulman Page P C and Meech S R 2013 *Faraday Discuss.* 163 277
- [18] Mitra R D, Silva C M and Youvan D C 1996 *Gene* 173 13
- [19] Mauring K, Krasnenko V and Miller S 2007 *J. Lumin* 122-123 291
- [20] Zhao L, Liu J Y and Zhou P W 2017 *Spectrochim. Acta, Part A* 186 52
- [21] Mauring K, Deich J, Rosell F I, McAnaney T B, Moerner W E and Boxer S G 2005 *J. Phys. Chem. B* 109 12976
- [22] Kummer A D, Wiehler J, Schüttigkeit T A, Berger B, Steipe B and Michel-Beyerle M E 2002 *ChemBioChem* 3 659
- [23] Fang X, Wang Y, Wang D, Zhao G, Zhang W, Ren A, Wang H, Xu J, Gao B R and Yang W 2014 *J. Phys. Chem. Lett.* 5 92
- [24] Wu D, Guo W W, Liu X Y and Cui G 2016 *Chemphyschem* 17 2340
- [25] H. J. Werner, P. J. Knowles, G. Knizia, F. R. Manby, M. Schütz et al., MOLPRO, version 2010.1, a package of ab initio programs, 2010, see <http://www.molpro.net>.